Published in final edited form as:
*J Vasc Interv Radiol*. 2011 October ; 22(10): 1437–1446. doi:10.1016/j.jvir.2010.12.039.

# Challenging the Surgical Rodent Hindlimb Ischemia Model with the Miniinterventional Technique

**Zhen W. Zhuang, MD**, **Jing Shi, MD**, **John M. Rhodes, PhD**, **Michael J. Tsapakos, MD**, and **Michael Simons, MD**
Department of Internal Medicine, Section of Cardiovascular Medicine (Z.W.Z., J.M.R., M.S.), Yale University, 375 Congress Ave., LSOG 120C, New Haven, CT 06519; Medical Medium Systems (J.S.), West Lebanon; and Department of Radiology(M.J.T.), Dartmouth Medical School, Lebanon, New Hampshire

## Abstract

**Purpose—**To develop an interventional hindlimb ischemic model and compare its angiogenic effect versus surgical ligation (SL) and excision of the femoral artery in rats treated with transplantation of bone marrow mononuclear cells (MNCs) as an angiogenic stimulator.

**Materials and Methods—**Forty-eight Lewis rats randomly received interventional embolization (IE) with hydrogel wire or SL and excision of the right femoral artery. Rodents were intraarterially transplanted with $1.5 \times 10^7$ MNCs in 500 $\mu$L medium from 24 isogenic donor rats. Functional and structural recovery was evaluated by laser Doppler imaging (LDI), cytokine/chemokine assay, and histologic staining.

**Results—**In vivo microscopic images showed significantly dilated vasa vasorum around the embolized segment of the right femoral artery at 3 days compared with disorganized tissue structure in the SL group. However, the LDI index was significantly higher in the SL group at 3 days compared with the IE group. LDI did not significantly differ between the two groups at 2 weeks after transplantation. Cytokine assay showed higher levels of interleukin (IL)–1$\alpha$ and IL-18 in the SL group; the IE group had higher levels of interferon-$\gamma$, IL-6, IL-13, and granulocyte colony-stimulating factor. Histologic examination demonstrated inflammatory infiltration near the incision within nerve fibers with dilated capillaries, showing nerve degeneration in the SL group. At 2 weeks, histologic analysis demonstrated massive scarring under the skin spreading into the musculature in the SL group.

**Conclusions—**A minimally invasive hindlimb ischemia model has been successfully developed that preserves tissue integrity and minimizes inflammation and confounding factors in the early stages of angiogenesis and arteriogenesis.

The prevalence of lower-extremity peripheral arterial disease is approximately 10% in people younger than 65 years and increases to 20% in people older than 75 years in the United States (1). Restoration of blood flow through angiogenesis and arteriogenesis may provide “biological revascularization” in these patients (2). In the past decade, intensive efforts have been undertaken to achieve neovascularization of ischemic limbs through the administration of growth factors that promote angiogenesis and/or arteriogenesis. Numerous animal studies (3– 6) have shown the feasibility of enhancing vessel growth in ischemic



Address correspondence to Z.W.Z.; zhen.zhuang@yale.edu.

From the 2008 SIR Annual Meeting.

None of the authors have identified a conflict of interest.

tissues, and the clinical application of growth factors has shown encouraging results in several small studies (7).

Vascular endothelial growth factor (VEGF) plays an important role in the process of angiogenesis and promotes the proliferation and migration of endothelial cells (8); fibroblast growth factor is also a strong inducer of angiogenesis (9). In addition, it was recently demonstrated that VEGF and fibroblast growth factor had a synergistic effect on angiogenesis (10). However, two phase II randomized controlled clinical trials involving VEGF (11) and basic fibroblast growth factor (12) for intermittent claudication have not corroborated the results of these smaller studies.

Many issues may have contributed to the lack of success of clinical growth factor therapy (9,13). However, the problem may also result from inadequate animal models used in these animal studies. In particular, surgical ligation (SL) of the common femoral artery, frequently used as a model in such studies (4,5,14,15), may induce a number of artifacts as a result of extensive inflammatory injury that by itself can promote angiogenesis and alteration of the vascular bundle structure. Moreover, there is a persistent need for reliable noninvasive imaging techniques that allow monitoring of vessel development and function in response to therapy.

Animal models of human disease are a source of great insight, yet they also carry potentially crucial limitations that may confound experimental data. Useful models should incorporate the following essential features: (i) clinical relevance, (ii) low cost, (iii) small animal size, and (iv) provision of sufficient material for the study of cellular and molecular mechanisms. Rats meet these requirements, which ensure their popularity for models of vascular disease. However, the existing surgical hindlimb ischemic model is limited to surgical injury and wound healing in the targeted area. In addition, its clinical relevance to the anatomic and functional characteristics of intravascular atherosclerotic stenosis or occlusion is questionable. The present study addresses these issues through the development of an interventional hindlimb model, which compares the angiogenic effect versus SL and excision of the femoral artery in rats treated with bone marrow mononuclear cells (MNCs), an angiogenic stimulator (6).

We expect an interventional hindlimb model can not only preserve the tissue integrity, but also minimize inflammatory reaction from open surgery at the early stages and wound healing at the later stages, which will be conducive to the exploration of the cellular and molecular mechanisms in terms of functional and structural regeneration of blood vessels through pure angiogenesis and arteriogenesis.

## MATERIALS AND METHODS

### Animals

Seventy-two male inbred Lewis rats (weight, 250 –275 g; Harlan, Indianapolis, Indiana), 10 –12 weeks of age, were used for all experiments. By using an Internet-based source (http://randomizer.org/form.htm), 48 rats were randomly assigned to undergo interventional embolization (IE; n = 24) or SL (n = 24). The balance (n = 24) were saved as donors for MNCs. The study conformed to the Guide for the Care and Use of Laboratory Animals published by the National Institutes of Health (publication no. 85-23, revised 1985) and was approved by the institutional animal care and use committee.

### Hydrogel Coil in Vitro Study

The HydroCoil embolization system (MicroVention, Aliso Viejo, California) consists of a synthetic, polymeric hydrogel attached to a 0.014-inch platinum coil. Segments 10 mm long

were cut from the 10-mm × 20-cm complex helical platinum coils. Images were obtained with the M2Bio three-dimensional microscopy system while the coil was immersed in the rat's serum at six different time points: pre-immersion; 10 seconds; and 5, 10, 15, and 20 minutes post-immersion. Axiovision 4.2 software (Zeiss) was used to assess the diameters of the coil.

### Bone MNC Transplantation

Bone marrow was harvested from the femur and tibia of 24 isogenic Lewis donor rats and MNCs were isolated by Ficoll density gradient centrifugation (Lymphoprep; Nycomed, Zurich, Switzerland) as described previously (6). MNCs were used as a neovascular stimulus (6).

### Interventional Hindlimb Model in Rats

Rats were anesthetized with intramuscular ketamine hydrochloride 80 mg/kg and xylazine 10 mg/kg. Heparin 100 IU was administered intraperitoneally. By using the sterile technique and with the assistance of a binocular loupe (magnification ×4; World Precision Instruments, Sarasota, Florida), a midline incision was made along the neck. The left common carotid artery was exposed and ligated distally with 4 – 0 silk suture, and a proximal suture was used to control bleeding during incision. A 2.4-F catheter over a 0.014-inch guide wire (Guidant, Santa Clara, California) was inserted into the incision and advanced to the proximal portion of the common femoral artery under C-arm fluoroscopic guidance (OEC 9900 Elite C-arm; GE Medical Systems, Milwaukee, Wisconsin). An angiogram was obtained with use of 0.5 mL Ultravist (Berlex, Wayne, New Jersey) to save as a roadmap. One 10-mm HydroCoil segment was loaded manually into a polyethylene tube (PE-50). This tube was opposite to the hub of the indwelling 2.4-F catheter. The coil segment was introduced into the artery with the same guide wire. The distal end of the coil segment was positioned approximately 2– 4 mm proximal to the bifurcation of the popliteal and saphenous arteries. The catheter was then pulled back to the abdominal aorta. Complete occlusion of the artery was confirmed by injection of 0.5 mL Ultravist for angiography 20 minutes later. Then, $1.5 \times 10^7$ MNCs in 500 $\mu$L Dulbecco's modified Eagle medium was injected through the same catheter positioned proximal to the bifurcation of the internal and external iliac artery, followed by another 500 $\mu$L Dulbecco's modified Eagle medium for flush. The incision was sutured in layers with a 4 – 0 silk suture. Twenty-two of 24 interventionally successful rats were randomly assigned to one of three groups according to follow-up time: group 1 (n = 5; days 3 and 14) for in vivo microscopic imaging and histologic study; group 2 (n = 6; day 7) for cytokine measurement; and group 3 (n = 11; day 14) for laser Doppler imaging (LDI).

### Surgical Hindlimb Ischemia Model

Surgical procedures were performed in 24 rats under anesthesia and sterile conditions. A vertical longitudinal incision was made in the right hindlimb (2–3 cm long). The right femoral artery and its side branches were dissected and ligated with 4 – 0 silk sutures spaced 10 mm apart, and the vessel segment between the ligatures was excised. By using the same technique as described in the previous section, $1.5 \times 10^7$ MNCs in 500 $\mu$L Dulbecco's modified Eagle medium were transplanted in the bifurcation of the internal and external iliac artery via a transcarotid access.

The rats were randomly assigned to one of three groups according to follow-up time: group 4 (n = 6; days 3 and 14) for in vivo microscopic imaging and histologic study; group 5 (n = 6; day 7) for cytokine assay; and group 6 (n = 12; day 14) for LDI.

### Multiplex Assays Specific for Rat Cytokines and Chemokines

In group 2 (IE; n = 6) and group 5 (SL; n = 6), an intravenous catheter (PE-50) for sampling blood from the ischemic hindlimb was inserted and positioned at the iliac vein bifurcation through the right external jugular vein under fluoroscopic guidance. This catheter and the occluder were tunneled subcutaneously and exteriorized between the scapulas. Time points for blood sampling included before arterial occlusion and days 1, 3, 5, and 7 after the procedure. At each time point, 0.5 mL blood was drawn and 0.5 mL saline solution was supplied for flush. In preparing serum samples, blood, collected in a sterile tube, was allowed to clot for 30 minutes at minimum before centrifugation for 10 minutes at 1,000*g*. Serum was removed immediately, divided into aliquots, and stored at −80 °C until cytokine assay.

Multiplexed immunoassays with the use of fluorescent microspheres and the Luminex-100 system (Luminex, Austin, Texas) were performed on 60 samples of serum in six IE-group rats and six SL-group rats. Multianalyte profiling was performed on the Luminex-100 system, and acquired fluorescence data were analyzed by MasterPlex QT software (version 1.2; MiraiBio, San Francisco, California). Serum concentrations of the following 24 cytokines/chemokines were simultaneously quantified by using the multiplex assay kit (cat. RCYTO-80K) per the manufacturer's instructions: eotaxin, granulocyte colony-stimulating factor (GCSF), granulocyte–macrophage colony-stimulating factor, keratinocyte-derived chemokine/growth regulated oncogene, interferon (IFN)– $\gamma$, leptin, interleukin (IL)–1$\alpha$, IL-1$\beta$ IL-2, IL-4, IL-5, IL-6, IL-9, IL-10, IL-12p70, IL-13, IL-17, IL-18, IFN-inducible protein–10, monocyte che-moattractant protein-1, macrophage inflammatory protein–1$\beta$, regulated upon activation normal T cell expressed and secreted, tumor necrosis factor–$\alpha$, and VEGF.

### Assessment of Blood Perfusion by LDI

We scanned the rear paw and the front side of the thigh for rats in groups 3 and 6 with an LDI analyzer (Moor Instrument, Wilmington, Delaware) before and after the interventional or surgical procedure (days 0, 3, 7, and 14). This method has been validated extensively in rodent models of hindlimb ischemia and is considered a reference standard for perfusion assessment (4,15,16). Measurement of blood flow with LDI has been previously described (16). Low or no perfusion is displayed as dark blue, whereas the highest degree of perfusion is displayed as red. These images were quantitatively converted into histograms that represented the amount of blood flow on the x-axis and the number of pixels on the y-axis in the traced area. The average blood flow in each histogram was calculated and the LDI index was determined as the ratio of ischemic to nonischemic hindlimb blood perfusion.

### Histologic Analysis

Six rats (n = 3 in groups 1 and 4) were anesthetized as mentioned previously at day 3 and an additional five rats (n = 2 in group 1 and n = 3 in group 4) were anesthetized at day 14. Under binocular loupe guidance, the arterial region was visualized and digitally photographed after a vertical longitudinal incision was made in the right hindlimb. These rats were killed with an overdose of ketamine and xylazine. At necropsy, adductor muscles and the region including nerve, artery, and vein with surrounding tissue were harvested separately. These structures were cut into 5-mm-thick blocks and the coil segments were carefully extracted from the femoral artery. After paraffin embedding, 6-$\mu$m-thick sections were cut from each sample with muscle fibers oriented in the transverse direction, stained with hematoxylin and eosin, examined at magnifications of ×100 or ×400, and analyzed by the research core service from the department of pathology for tissue response to different intervention.

### Statistical Analysis

Data were expressed as means ± SD. Measurements of LDI and cytokines were compared between two models (SL vs IE) with unpaired Student *t* test by using SPSS version 11.0 software (SPSS, Chicago, Illinois), with differences significant at $P < .05$.

## RESULTS

### Operation Technique and Postoperative Recovery

The operation success rates were 100% (n = 24) for the SL model and 92% (n = 22) for the IE model (Fig 1). Of the two animals in the IE group who were excluded from further studies (one in group 1, the other in group 3), one had a misembolization and the other had a vascular spasm attributable to malpositioning of the guide wire and catheter. After both procedures, the animals recovered well and there were no distal tissue losses.

### Hydrogel Coil in Vitro Study

The initial diameter of the hybrid HydroCoil was 0.014 inches. During the first 5 minutes, the diameter increased dramatically to approximately 0.032 inches. The coil expanded moderately but gradually until the total outer diameter reached 0.040 inches (Fig 2). Our bench data suggested that the time frame for repositioning (ie, partial deployment and retraction back into the catheter) is limited to 5 minutes.

### Blood Flow Recovery

LDI was used to measure blood flow in the foot and upper leg in both groups to 14 days after embolization or after ligation and excision (Figs 3, 4). For the rats in the IE group, blood flow was lowest at the foot immediately after embolization (21.6% ± 1.4) and recovered to 58.2% ± 8.2 at day 3. Blood flow recovered more slowly during the resting period at day 14, achieving a final ratio of 88.6% ± 8.8. Conversely, a different pattern of blood flow recovery occurred in rats from the SL group: blood flow recovered much faster compared with the IE group at day 3 (74.6% vs 58.2%; $P < .01$). There were no significant differences at any other time points ($P > .05$; Fig 3b).

SL led to decreased arterial and venous blood flow signals with disruption of flow around the incision as determined by LDI. Images from the same surgical area clearly showed hyperemia around the excised artery 3 days later that regressed by day 7. In contrast to this finding, the IE model clearly demonstrated that perfusion imaging gradually recovered with intact venous signal (Fig 4).

### Histologic Findings

In vivo microscopic images demonstrated that tissue integrity was maximally preserved in the IE model on day 3. In addition, the femoral nerve, artery, and vein were not damaged. In response to the blockage of the femoral artery, the vasa vasorum outside the blocked artery was substantially dilated. In contrast, the SL model clearly showed disordered structures in place of the vacant artery without visible vasa vasorum (Fig 5). On day 14, dilated vasa vasorum regressed to normal in the IE hindlimb. With the exception of the resulting scar, there was no histologic difference in the findings between days 3 and 14 in the SL hindlimb.

Histologic analysis showed a few inflammatory cells that penetrated into the femoral arterial wall (ie, adventitial layer) with hydrogel attached to the luminal side and no wire in the middle of lumen in the IE model on day 3 (Fig 6, middle). The accompanying nerve was intact. In comparison with the IE hindlimb, histologic evaluation of vasculature and musculature in the SL hindlimb showed that inflammatory cells spread inside the incision

and penetrated into the nerve fiber, causing slight nerve degeneration and dilation of capillaries (Fig 6, right).

On day 14, histologic images clearly showed neointima forming inside the embolized segment of the femoral artery as a result of constant stimulation of the hydrogel in the IE hindlimb (Fig 7a, left). In contrast, histologic evaluation of vasculature and musculature in the thigh of the SL hindlimb demonstrated disorganized scarring with inflammatory cells and dilated arterioles occupying the space of the excised artery (Fig 7a, right). In addition, inflammatory cells also migrated into the musculature, extending the scar formation Fig 7b).

### Inflammatory Cytokines

Measurements of serum proinflammatory cytokine levels demonstrated distinct differences between the two groups. The SL group had higher levels of IL-1$\alpha$ and IL-18, whereas the IE group had higher levels of INF-$\gamma$, IL-6, IL-13, and GCSF (Fig 8). There was no difference between the two models with regard to the rest of cytokines not mentioned.

## DISCUSSION

In the present study, we show that an interventional rather than a surgical method of hindlimb ischemia induction preserves tissue integrity around the site of arterial occlusion and leads to a distinctly different serum cytokine profile and pattern of flow recovery.

Hindlimb ischemia can be induced successfully in rats by using a catheter-based technique with a low-profile expandable hydrogel–platinum coil. This hydrogel coil offers all the favorable attributes of currently available platinum coils, including ready passage through microcatheters, radiopacity, atraumatic deployment, and retrievability. For regular coil embolization, incomplete initial occlusion rates and late re-establishment of patency are two major limitations (17). The mechanisms likely relate to thrombolysis and recanalization of thrombus that are initially induced by these kinds of coils (17). However, the hydrogel coil overcomes both of these important shortcomings. The lumen treated with the hydrogel coil is completely occluded, similar to SL. This has been demonstrated by in vivo angiography (20 min after delivery) and quantitative LDI data. Histologic evidence further confirms the intraluminal occlusion and neointimal development. To the contrary, the expanded hydrogel excludes thrombus, although some blood cells are trapped within the expanded hydrogel, eradicating the tendency for recanalization. This is its unique characteristic that has been applied clinically (18). Our findings suggest that IE caused rapid and complete blood flow blockage, similar to SL and excision.

This model has advantages versus a standard surgical approach in the absence of nerve stimulation or venous dissection around the occluded artery and maximal preservation of tissue integrity. In contrast, during surgical arterial resection, the neural networks were often injured when the common femoral artery was exposed, dissected, and ligated. We observed that the nerve bundle was displaced in the surgical hindlimb model at day 3 (n = 3 per group). In addition, inflammatory cells penetrated into the nerve fibers, and the capillaries within these bundles were dilated. In contrast, the neural network was kept intact and still coursed along the vessel in an orderly pattern in our IE model. There was no evidence of inflammatory reaction inside the nerve bundle. Although not addressed in the present study, nerves are a major source of VEGF (19) and play an important guiding role in arterial development (20). Our results suggest that no difference in VEGF levels was found between the two models.

In addition, preexisting collateral vessels and vasa vasorum within the adventitia were frequently interrupted and the nearby femoral vein was also injured by the surgical

procedure. There is considerable evidence indicating participation of the adventitia vasculature and veins in arterial neovascularization (21,22). Our observation that vasa vasorum dilation compensated for the occlusion of the embolized conductance artery is consistent with the role of adventitial vasculature in arteriogenesis. In contrast, vasa vasorum tends to disappear in our SL model, implying damage to this important structure. Currently, SL and excision of the femoral artery are the reference standard for the creation of durable, complete occlusions in the hindlimb ischemia model (23–26).

In some studies, both the femoral artery and vein are dissected and excised (27–29). However, such an extensive resection and substantial injury results in extensive release of various growth factors such as basic and acidic fibroblast growth factors, and severe tissue ischemia leads to high local VEGF production. The extensive accumulation of these factors may seriously compromise the preclinical efficacy study, unintentionally adding a potent mix of angiogenic growth factors to a therapeutic molecule. Clearly, this is not a situation encountered in patients in therapeutic angiogenesis trials. In addition, extensive injury encourages recruitment of peripheral blood MNCs that can further stimulate arteriogenesis by secreting pro- and antiinflammatory cytokines, which might mediate endothelial cell activation, migration, proliferation, and apoptosis (30). In the surgical model, serum proinflammatory cytokine levels (eg, IL-1$\alpha$, IL-18) were significantly increased without alteration of the level of antiinflammatory cytokines. IL-1 $\alpha$ is primarily involved in regulating intracellular events and is a mediator of local inflammation. In addition, it promotes angiogenesis in vivo, and the presence of an inflammatory environment is essential for its angiogenic activities (31). Meanwhile, IL-18 has proinflammatory and angiogenic effects (32).

In contrast to surgical hindlimb arterial occlusion, IE with hydrogel coil results in a distinctly different serum cytokine profile with an increase in proinflammatory IFN-$\gamma$, antiinflammatory IL-6 and IL-13, and GCSF. IFN-$\gamma$ inhibits not only the growth of endothelial cells, but also angiogenesis (33). IL-6 secreted by lymphocytes and monocytes and IL-13 secreted by T helper cells have antiinflammatory activities by attenuating macrophage function. GCSF plays a critical role in the regulation of proliferation, differentiation, and survival of bone marrow progenitor cells. GCSF also mobilizes hematopoietic stem cells into the peripheral blood circulation (34). The blood flow recovered much faster in rats from the SL group than rats in the IE group at the early stage (day 3), which can be partially explained by increased proinflammatory cytokines (IL-1$\alpha$ and IL-18). At the intermediate stage (day 7), the difference in blood flow recovery pattern noted with LDI diminished, but blood flow consistently recovered. This may be a result of the balance between pro- and antiinflammatory cytokines at higher levels than at the early stage. At 2 weeks after the procedure, the net effect of pro- and antiinflammatory components in our interventional hindlimb models tends to be proangiogenic, as data from LDI and histologic study showed no difference between the two groups.

Angiogenesis and arteriogenesis in adult tissues are complex processes involving multiple growth factors, receptors, cytokines/chemokines, extracellular matrix, complex intracellular signaling pathways, and perhaps local and bone marrow– derived endothelial progenitor cells (35). We speculate that different hindlimb ischemia models might induce different cytokines/chemokines, which may promote different angiogenic and arteriogenic pathways. We further speculate that the severe inflammation, nerve stimulation, and venous trauma occurring in an SL hindlimb model create a proarteriogenic environment at an early stage, which may explain active arteriogenesis and the straightforward response to therapeutic angiogenesis interventions in animal studies. The lack of this proarteriogenic environment in the setting of chronic human peripheral arterial disease may explain the failure of gene therapies to adequately reverse human critical limb ischemia (11,12).

An important limitation of the present study was that MNCs were not labeled, so their potential of differentiation into vascular-forming cells could not be identified by molecular imaging or immunohistochemistry.

We have developed a clinically relevant rodent hindlimb model by embolizing the common femoral artery with a hydrogel wire. In contrast to existing hindlimb models, our model allows controlled, uniform, and reproducible blockage of the conduit vessel without edema and wound injury, minimizing the inflammatory reaction to the surrounding tissue and eliminating the wound healing process. Besides its general utility in probing the mechanisms of angiogenesis and arteriogenesis, this model is uniquely applicable to studies seeking to relate histologic to genomic outcomes.

### Practical Applications

The mini-IE model that simulates human peripheral arterial disease as closely as possible appears to be promising for the study of true therapeutic angiogenesis and arteriogenesis. This method could be adequate for the establishment of ischemic models in other vascular diseases, such as focal cerebral ischemia and coronary infarction. In addition, bone marrow–derived MNC sources and cell preparations were used in this study, in which encouraging results might provide the rationale for clinical trials to administer MNCs intraarterially to patients with atherosclerotic peripheral arterial disease. The emerging field of therapeutic arteriogenesis may benefit from quantitative LDI because it enables serial assessment of muscle ischemia noninvasively and without x-ray exposure.

## Acknowledgments

Z.W.Z. was supported by a Society of Interventional Radiology Foundation grant.

The assistance and formatting of this manuscript by Carol Akirav are gratefully acknowledged.

## ABBREVIATIONS

| | |
|---|---|
| **GCSF** | granulocyte colony-stimulating factor |
| **IE** | interventional embolization |
| **IFN** | interferon |
| **IL** | interleukin |
| **LDI** | laser Doppler imaging |
| **MNC** | mononuclear cell |
| **SL** | surgical ligation |
| **VEGF** | vascular endothelial growth factor |

## References

1. Criqui MH, Fronek A, Barrett-Connor E, Klauber MR, Gabriel S, Goodman D. The prevalence of peripheral arterial disease in a defined population. Circulation. 1985; 71:510–515. [PubMed: 3156006]
2. Rosengart TK, Patel SR, Crystal RG. Therapeutic angiogenesis: protein and gene therapy delivery strategies. J Cardiovasc Risk. 1999; 6:29–40. [PubMed: 10197290]
3. Post MJ, Sato K, Murakami M, et al. Adenoviral PR39 improves blood flow and myocardial function in a pig model of chronic myocardial ischemia by enhancing collateral formation. Am J Physiol Regul Integr Comp Physiol. 2006; 290:R494–R500. [PubMed: 16254127]

4. Tirziu D, Moodie KL, Zhuang ZW, et al. Delayed arteriogenesis in hypercholesterolemic mice. Circulation. 2005; 112:2501–2509. [PubMed: 16230502]
5. Yu J, deMuinck ED, Zhuang Z, et al. Endothelial nitric oxide synthase is critical for ischemic remodeling, mural cell recruitment, and blood flow reserve. Proc Natl Acad Sci U S A. 2005; 102:10999–1004. [PubMed: 16043715]
6. Zhuang ZW, Gao L, Murakami M, et al. Arteriogenesis: noninvasive quantification with multi-detector row CT angiography and three-dimensional volume rendering in rodents. Radiology. 2006; 240:698–707. [PubMed: 16926325]
7. Manninen HI, Makinen K. Gene therapy techniques for peripheral arterial disease. Cardiovasc Intervent Radiol. 2002; 25:98–108. [PubMed: 11901426]
8. Ferrara N, Davis-Smyth T. The biology of vascular endothelial growth factor. Endocr Rev. 1997; 18:4–25. [PubMed: 9034784]
9. Simons M. Angiogenesis: where do we stand now? Circulation. 2005; 111:1556–1566. [PubMed: 15795364]
10. Kano MR, Morishita Y, Iwata C, et al. VEGF-A and FGF-2 synergistically promote neoangiogenesis through enhancement of endogenous PDGF-B-PDGFRbeta signaling. J Cell Sci. 2005; 118:3759–3768. [PubMed: 16105884]
11. Rajagopalan S, Mohler ER 3rd, Lederman RJ, et al. Regional angiogenesis with vascular endothelial growth factor in peripheral arterial disease: a phase II randomized, double-blind, controlled study of adenoviral delivery of vascular endothelial growth factor 121 in patients with disabling intermittent claudication. Circulation. 2003; 108:1933–1938. [PubMed: 14504183]
12. Lederman RJ, Mendelsohn FO, Anderson RD, et al. Therapeutic angiogenesis with recombinant fibroblast growth factor-2 for intermittent claudication (the TRAFFIC study): a randomised trial. Lancet. 2002; 359:2053–2058. [PubMed: 12086757]
13. Simons M, Ware JA. Therapeutic angiogenesis in cardiovascular disease. Nat Rev Drug Discov. 2003; 2:863–871. [PubMed: 14668807]
14. Waters RE, Terjung RL, Peters KG, Annex BH. Preclinical models of human peripheral arterial occlusive disease: implications for investigation of therapeutic agents. J Appl Physiol. 2004; 97:773–780. [PubMed: 15107408]
15. Luo F, Wariaro D, Lundberg G, Blegen H, Wahlberg E. Vascular growth factor expression in a rat model of severe limb ischemia. J Surg Res. 2002; 108:258–267. [PubMed: 12505050]
16. Morishita R, Sakaki M, Yamamoto K, et al. Impairment of collateral formation in lipoprotein(a) transgenic mice: therapeutic angiogenesis induced by human hepatocyte growth factor gene. Circulation. 2002; 105:1491–1496. [PubMed: 11914260]
17. Tamatani S, Ozawa T, Minakawa T, Takeuchi S, Koike T, Tanaka R. Radiologic and histopathologic evaluation of canine artery occlusion after collagen-coated platinum microcoil delivery. AJNR Am J Neuroradiol. 1999; 20:541–545. [PubMed: 10319955]
18. Canton G, Levy DI, Lasheras JC. Changes in the intraaneurysmal pressure due to HydroCoil embolization. AJNR Am J Neuroradiol. 2005; 26:904–907. [PubMed: 15814942]
19. Mukouyama YS, Shin D, Britsch S, Taniguchi M, Anderson DJ. Sensory nerves determine the pattern of arterial differentiation and blood vessel branching in the skin. Cell. 2002; 109:693–705. [PubMed: 12086669]
20. Carmeliet P, Tessier-Lavigne M. Common mechanisms of nerve and blood vessel wiring. Nature. 2005; 436:193–200. [PubMed: 16015319]
21. Madrid JF, Diaz-Flores L, Gutierrez R, et al. Participation of angiogenesis from rat femoral veins in the neovascularization of adjacent occluded arteries. Histol Histopathol. 1998; 13:1–11. [PubMed: 9476628]
22. Khurana R, Zhuang Z, Bhardwaj S, et al. Angiogenesis-dependent and independent phases of intimal hyperplasia. Circulation. 2004; 110:2436–2443. [PubMed: 15477408]
23. Iglarz M, Silvestre JS, Duriez M, Henrion D, Levy BI. Chronic blockade of endothelin receptors improves ischemia-induced angiogenesis in rat hindlimbs through activation of vascular endothelial growth factor-no pathway. Arterioscler Thromb Vasc Biol. 2001; 21:1598–603. [PubMed: 11597932]

24. Mohler ER 3rd, Sehgal CM, Ferrari VA, Parmacek M, Shih A, Wilensky RL. A novel ultrasound method for evaluation of collateral development in limb ischemia. Vasc Med. 2002; 7:169–175. [PubMed: 12553739]
25. Paoni NF, Peale F, Wang F, et al. Time course of skeletal muscle repair and gene expression following acute hind limb ischemia in mice. Physiol Genomics. 2002; 11:263–272. [PubMed: 12399448]
26. Cao R, Brakenhielm E, Pawliuk R, et al. Angiogenic synergism, vascular stability and improvement of hind-limb ischemia by a combination of PDGF-BB and FGF-2. Nat Med. 2003; 9:604–613. [PubMed: 12669032]
27. Duan J, Murohara T, Ikeda H, et al. Hyperhomocysteinemia impairs angiogenesis in response to hindlimb ischemia. Arterioscler Thromb Vasc Biol. 2000; 20:2579–2585. [PubMed: 11116056]
28. Sasaki K, Duan J, Murohara T, et al. Rescue of hypercholesterolemia-related impairment of angiogenesis by oral folate supplementation. J Am Coll Cardiol. 2003; 42:364–372. [PubMed: 12875777]
29. Iwase T, Nagaya N, Fujii T, et al. Adrenomedullin enhances angiogenic potency of bone marrow transplantation in a rat model of hindlimb ischemia. Circulation. 2005; 111:356–362. [PubMed: 15655128]
30. Lingen MW. Role of leukocytes and endothelial cells in the development of angiogenesis in inflammation and wound healing. Arch Pathol Lab Med. 2001; 125:67–71. [PubMed: 11151055]
31. Salven P, Hattori K, Heissig B, Rafii S. Interleukin-1alpha promotes angiogenesis in vivo via VEGFR-2 pathway by inducing inflammatory cell VEGF synthesis and secretion. FASEB J. 2002; 16:1471–1473. [PubMed: 12205052]
32. Park CC, Morel JC, Amin MA, Connors MA, Harlow LA, Koch AE. Evidence of IL-18 as a novel angiogenic mediator. J Immunol. 2001; 167:1644–1653. [PubMed: 11466388]
33. Sato N, Nariuchi H, Tsuruoka N, et al. Actions of TNF and IFN-gamma on angiogenesis in vitro. J Invest Dermatol. 1990; 95(suppl):85S–89S. [PubMed: 1701814]
34. Joseph J, Rimawi A, Mehta P, et al. Safety and effectiveness of granulocyte-colony stimulating factor in mobilizing stem cells and improving cytokine profile in advanced chronic heart failure. Am J Cardiol. 2006; 97:681–684. [PubMed: 16490437]
35. Aviles RJ, Annex BH, Lederman RJ. Testing clinical therapeutic angiogenesis using basic fibroblast growth factor (FGF-2). Br J Pharmacol. 2003; 140:637–646. [PubMed: 14534147]

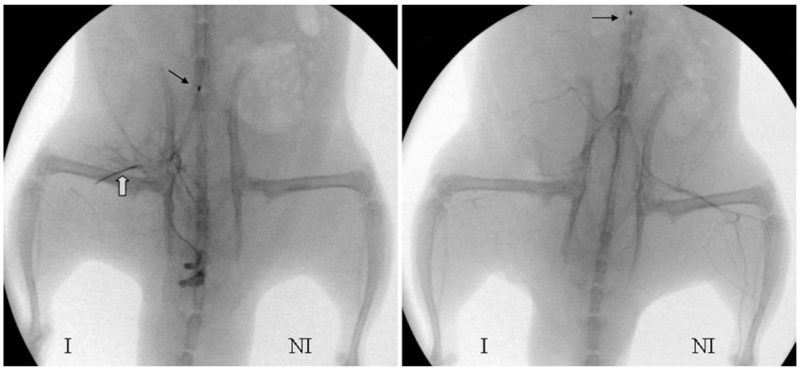


**Figure 1.**
Representative angiograms obtained 20 minutes after coil placement or SL and excision confirmed complete occlusion of the femoral artery. Left: Tip of a 2.4-F balloon catheter situated at the bifurcation of the right iliac artery. White arrow indicates 10-mm long hydrogel coil. Right: The coil is marked by the white arrow. Left: Tip of the same catheter located at the abdominal aorta. Small black arrow indicates the metal marker in the balloon catheter. (*I,* ischemia; *NI,* no ischemia.)

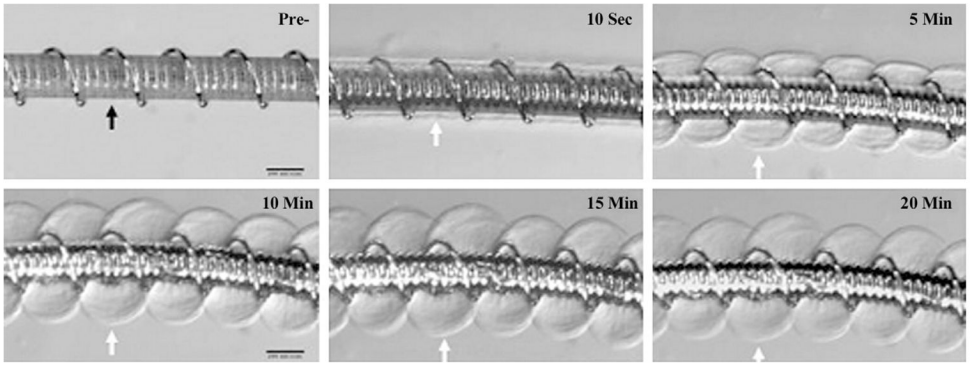


**Figure 2.**

HydroCoil device. Top left: Prehydration image shows initial profile (0.014 inches). Highly compact hydrogel material was wrapped around a platinum coil (black arrow). Indentations between platinum helical coils could be seen through the hydrogel polymer. The other images are posthydration images of the system soaked in rat serum at different time points, which show marked expansion of the hydrogel polymer, which had become translucent. The outer edges of the hydrogel are denoted by white arrows. (Scale bars: 200 $\mu$m.)

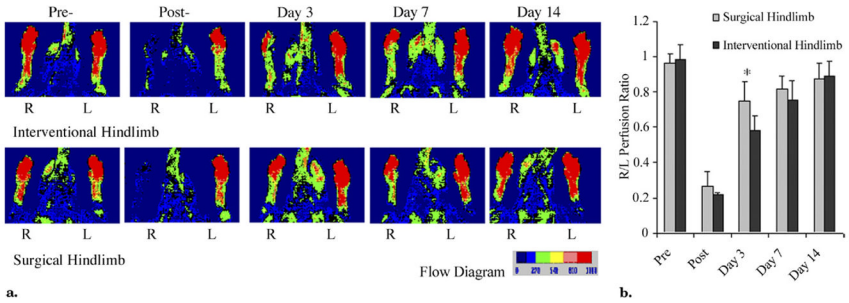


**Figure 3.**

LDI analysis of hindlimb perfusion in MNC-treated rats who had undergone an IE or SL procedure. **(a)** Representative LDI recorded before and at serial times after the femoral artery blockage in right (*R*) and left (*L*) foot. LDI-revealed perfusion ratios over time (right/left): SL (bottom row), 0.97 versus 0.13 versus 0.74 versus 0.71 versus 0.92; IE (top row), 1.00 versus 0.20 versus 0.56 versus 0.73 versus 1.00. The color scale of blood flow variations ranges from minimal (dark blue) to maximal (red). **(b)** Changes in perfusion shown as ratio of right to left hindlimb in SL-treated hindlimbs (gray bars) and IE-treated hindlimbs (black bars). Data shown as means ± SD; n = 11 rats in the IE group and n = 12 in the SL group (**P* < .01, SL vs IE).

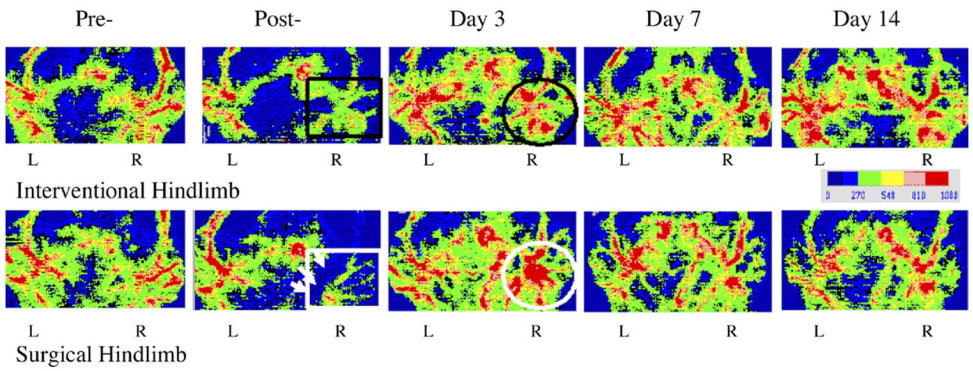


**Figure 4.**

Representative LDI at serial times after hydrogel wire embolization (top row) and SL (bottom row). Top row: Perfusion images after the procedure show decreased perfusion along the arterial course with intact venous signal (black rectangle). Image at day 3 demonstrated substantial blood flow recovery (black circle). Bottom row: Postperfusion image shows incision as dark blue area (white arrows) with significant decreased signals for artery and vein (white rectangle). However, after 3 days, imaging clearly demonstrated local hyperemia around excised artery (white circle). Day 7 image showed regression of local hyperemia.

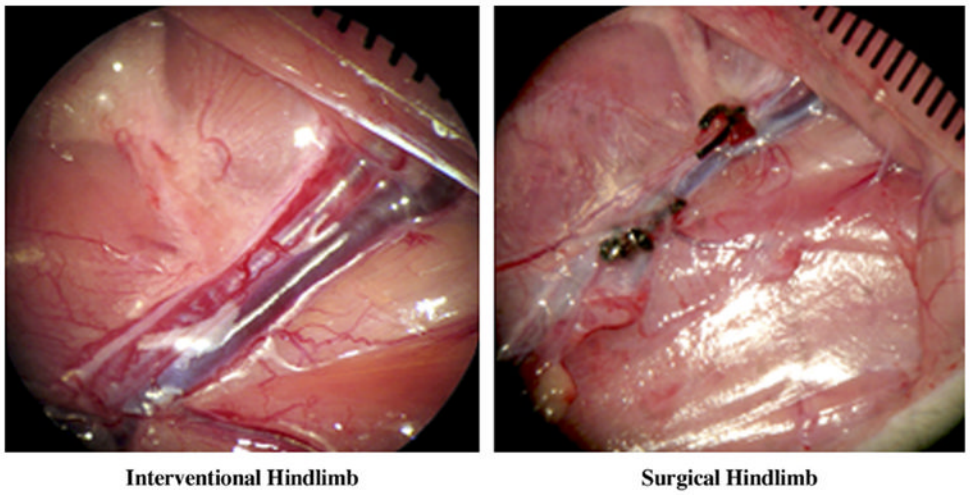


**Figure 5.**
Representative microscopic images 3 days after intervention (left) and surgery (right). Left: In vivo microscopic image shows significantly dilated vasa vasorum around embolized segment of the right femoral artery with intact structure (normal order: nerve, artery, and vein; shiny reflection within the artery came from the platinum coil and hydrogel). Right: In contrast to the IE-treated hindlimb, the SL-treated hindlimb displayed a displaced nerve and vacant artery between two sutures without dilated vasa vasorum. (Available in color online at www.jvir.org).

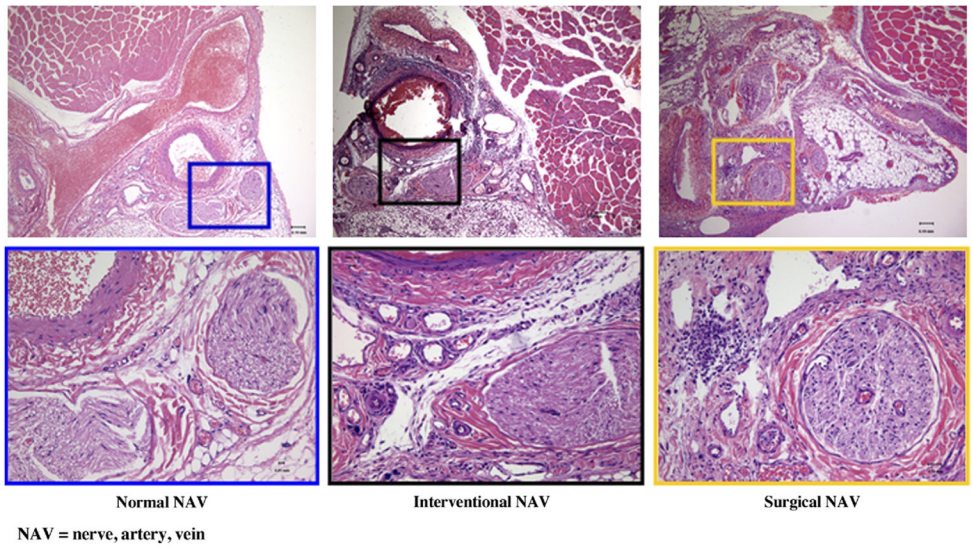


**Figure 6.**
Representative histologic images at 3 days after SL (right) and IE (middle) hindlimb treatment. Left: Normal targeted area that served as control. The IE-treated hindlimb showed limited inflammation with swelled hydrogel attaching to the vascular wall. In comparison with the IE hindlimb, histologic evaluation of vasculature and musculature in the upper leg of the SL-treated hindlimb at 3 days demonstrated inflammatory infiltration inside the incision, especially within the nerve bundle, with dilated capillaries and slight degeneration. (Hematoxylin and eosin stain; original magnification, × 10 [upper] and × 40 [lower].) (Available in color online at www.jvir.org).

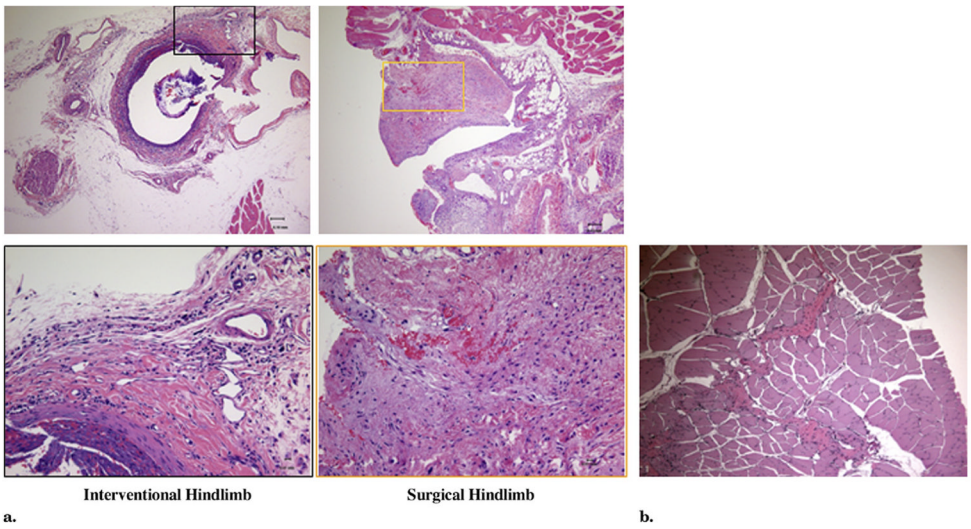


**Figure 7.**

**(a)** Representative histologic images 2 weeks after IE (left) and SL (right). The IE-treated hindlimb showed limited inflammatory cells surrounding the embolized artery. Within the lumen, neointima developed as a result of hydrogel stimulation with the remains of the hydrogel and vacant wire. The SL-treated hindlimb showed a scar under the incision. Within the scar, the inflammatory cells spread everywhere with dilated arterioles. **(b)** Inflammatory cells penetrated into the musculature and contributed to scar development. (Hematoxylin and eosin stain; original magnification, × 10 [upper] and × 40 [lower].) (Available in color online at www.jvir.org).

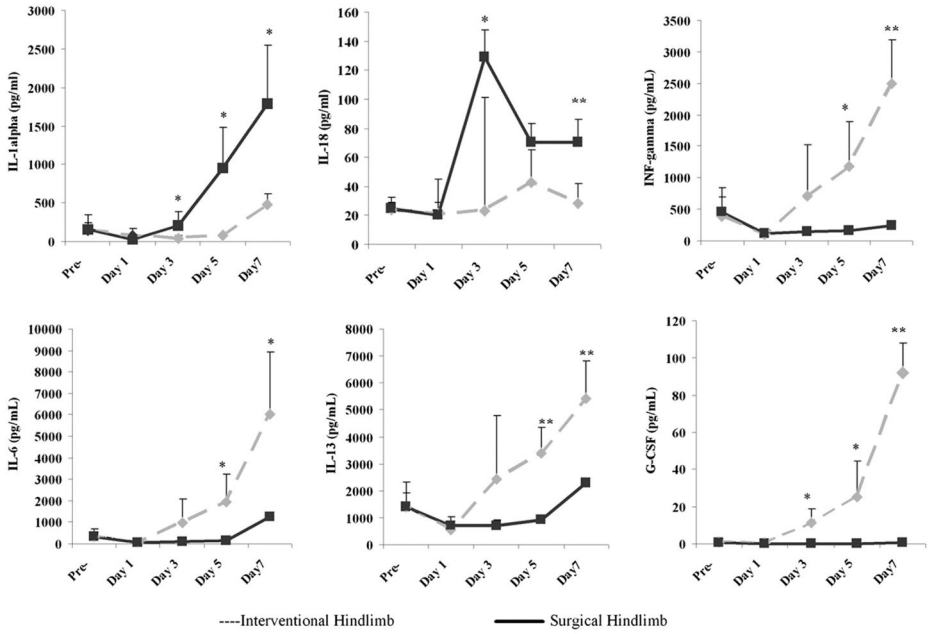


**Figure 8.**

Levels of proinflammatory cytokines IL-1$\alpha$, IL-18, and INF-$\gamma$ (upper), and antiinflammatory cytokines IL-6, IL-13, and GCSF (lower) in the serum differed after the induction of surgical or interventional ischemia. Results are presented as mean ± SD (*$P$ < .05, ** $P$ < .01; n = 6 rats per group per time point).